VSX J071108.7+695227: a Newly Discovered Short-period Eclipsing Binary

Mario Damasso
Astronomical Observatory of the Autonomous Region of the Aosta Valley, fraz. Lignan 39, 11020 Nus (Aosta), Italy; INAF associated; mario.damasso@studenti.unipd.it and m.damasso@gmail.com

and

Dept. of Physics and Astronomy, University of Padova, vicolo dell'Osservatorio 3, I-35122 Padova, Italy

Davide Cenadelli
Paolo Calcidese
Astronomical Observatory of the Autonomous Region of the Aosta Valley, fraz. Lignan 39, 11020 Nus (Aosta), Italy; INAF associated

Luca Borsato
Dept. of Physics and Astronomy, University of Padova, vicolo dell'Osservatorio 3, I-35122 Padova, Italy; INAF-OAPd associated

Valentina Granata
Dept. of Physics and Astronomy, University of Padova, vicolo dell'Osservatorio 3, I-35122 Padova, Italy

Valerio Nascimbeni
Dept. of Physics and Astronomy, University of Padova, vicolo dell'Osservatorio 3, I-35122 Padova, Italy; INAF-OAPd associated

Received March 28, 2012; revised April 13, 2012; accepted April 16, 2012

Abstract We report the discovery of an EW variable, VSX J071108.7+695227, with a short orbital period of ~0.238 day. This period is very close to the lower limit of ~0.22 day that has been found for EW systems. Here we present and discuss photometric and spectroscopic data of the variable, collected at the Astronomical Observatory of the Autonomous Region of the Aosta Valley and at the Asiago Astrophysical Observatory. The light curves show some asymmetries and the spectra suggest a dK4 classification for the two components. It could be interesting to carry out further observations of this system at different epochs because such systems frequently show variations in period and in the features of the light curve.

1. Introduction

We report the discovery of VSX J071108.7+695227 (= 2MASS J0711 0876+6952276), a short-period eclipsing binary system. We classify it as an EW type variable. This variable, located in the constellation Camelopardalis (R.A. 07^h 11^m 08.76^s; Dec. +69° 52' 27.6"; epoch J2000.0), was discovered thanks to photometric observations performed at the Astronomical Observatory of the Autonomous Region of the Aosta Valley (OAVdA), and at the Asiago Observatory. The system has an estimated orbital period of ~0.238 day.

The variable deserves further investigation mostly because the assessed period is very short and pretty close to the sharp cut-off at the lower limit of ~0.22 day found by Norton *et al.* (2011) for these binaries. Only a minor percentage of EW variables have periods shorter than ours. For example, Rucinski (2006) found that only a few tens out of the 4,638 EW systems of the ASAS sample have a period shorter than or similar to ours, Weldrake *et al.* (2007) found only two out of fifty-eight short period eclipsing binaries to have $P < 0.238$ day, and Miller *et al.* (2010) about ten out of 533. To date, the largest sample of EW systems with a period shorter than ours is made up of the fifty-three EW binaries with $P < 0.2314$ day listed by Norton *et al.* (2011). Moreover, such close systems show several features that change over time, as the orbital period and the shape of the light curves, as we discuss below.

All this considered, we pursued a photometric and spectroscopic analysis of our variable aimed at better characterizing its physical properties. We determined B, V, and R light curves, we assigned the two components to a spectral type, we looked for possible activity indicators in the spectra like emission lines, and we sought asymmetries in the light curves.

2. Instrumentation and methodology

Since the end of 2008, at the OAVdA is underway the implementation of an extensive observational campaign aimed at finding small-sized extrasolar planets around M dwarfs using the photometric transit method (Damasso *et al.* 2010; Giacobbe *et al.* 2012). The first observations of VSX J071108.7+695227 were perfomed at the end of December 2011, during the commissioning tests of the new telescope array which will be used for a five-year survey of hundreds of M dwarfs in the solar neighborhood. The array is composed of four identical 40-cm *f*/8.4 Ritchey-Chrétien telescopes, each on a 10 MICRON QCI2000 mount and equipped with a FLI ProLine 1001E CCD camera.

After the discovery, we photometrically followed up on the binary system with the main telescope present in OAVdA, an 81-cm f/7.9 Ritchey-Chrétien coupled to a back-illuminated CCD camera FLI ProLine PL 3041-BB and standard BVRI filters. The sensor is 2048 px × 2048 px, with a pixel area of 15×15 μm^2. The system has a FoV of 16.5×16.5 $arcmin^2$ with a

plate scale of 0.48"/pixel (binning 1 × 1). We present and discuss here the data collected with this telescope. In Figure 1 we present one of our frames and indicate our system.

2.1. Photometric data

The scientific frames taken during the discovery night and the follow-up observations were reduced and analyzed with the software package TEEPEE (Transiting ExoplanEts PipElinE) developed by some of the authors. A detailed description of the basic functions of the TEEPEE pipeline is provided in Damasso *et al.* (2010). In short, the final result of the data processing is the generation of the differential light curves of all the stars in the CCD field which were automatically recognized in every frame of the series. The ensemble photometry is obtained testing up to twelve apertures. The best set of comparison stars is automatically determined for a pre-selected target from a list of the 100 brightest objects found in the field, excluding the ones too close to the CCD borders. The aperture and set of reference stars selected at the end of the data processing are the ones which give the smallest RMS for the entire light curve of the object of interest.

Figure 2 (a, b, c) shows the normalized differential light curves of VSX J071108.7+695227 obtained in B, V, and R filters on January 16, 2012, during the follow-up observations with the 81-cm telescope. The differential magnitudes are calculated as the difference between the average instrumental magnitudes of the comparison stars and the instrumental magnitudes of the variable star. The comparison stars automatically selected by the TEEPEE pipeline for each filter are listed in Table 2. The light curves clearly unveil the EW variability type for the object and the observations cover almost 1.75 times the orbital period of the two components of the system, which we estimated to be ~0.238 day using the Fast Chi-Squared algorithm described in Palmer (2009) and freely available at http://public.lanl.gov/palmer/fastchi.html. Figure 3 shows the normalized V-band light curve folded according to the orbital period. The zero epoch is HJD(0) = 2455943.438.

We estimate a mean V magnitude for the object through the relations described in Pavlov (2009), which use the *J–K* color index from the *2MASS* catalogue (Skrutskie *et al.* 2006) and the U_f and U_a magnitudes from the *UCAC-3* catalogue (USNO 2012):

$$V_f = 0.531 \cdot (J–K) + 0.906 \cdot U_f + 0.95 \pm 0.08 \quad (1)$$

$$V_a = 0.529 \cdot (J–K) + 0.9166 \cdot U_a + 0.83 \pm 0.08 \quad (2)$$

Averaging the two values found from (1) and (2) results in $V = 14.37$, where $J = 12.631$, $K = 11.923$, $U_f = 14.366$, and $U_a = 14.396$.

Using the following conversion relations between the *USNO A2.0* (Monet *et al.* 1998) and Landolt BR magnitudes (Kidger 2003):

$$B = 1.097 \cdot \mathrm{USNO}(B) - 1.216 \quad (3)$$

$$R = 1.031 \cdot \mathrm{USNO}(R) - 0.417 \quad (4)$$

where USNO(B) = 14.8 and USNO(R) = 13.9, we obtained B = 15.0 and R = 13.9.

Moreover, the star also appears in the APASS catalogue (AAVSO 2012), which provides other estimates for B and V magnitudes: $B = 15.485 \pm 0.368$; $V = 14.468 \pm 0.289$.

2.2. Spectroscopic data

To better characterize the variable and look for possible activity indicators like emission lines, on January 26, 2012, we took nine consecutive spectra with the 182-cm Copernico telescope at the Asiago Observatory (http://www.pd.astro.it/asiago/), using the AFOSC CCD camera. Two different optical configurations were used (grism3 and grism8) with different dispersion and spectral coverage. The main features of these configurations are summarized in Table 1. We took five spectra using the grism3 and four with the grism8.

In Figure 3 we overplotted (solid and dashed) vertical lines corresponding to the orbital phases at which the nine spectra of the system were collected. It can be seen that the first ones (with both configurations) were taken at maximum brightness. They are shown in Figure 4. The other spectra do not show sizeable differences as compared to these, at least at the low dispersion accessible to us. It can be noticed, however, that they were taken at a not very different phase.

3. Discussion

At the epoch of our observations the light curves of the variable showed some clear asymmetries, as expected from such short-period systems. The most significant is an evident O'Connell Effect as the magnitude of the two maxima is different (Davidge and Milone 1984). The conventional way to assess the size of this effect is to measure the peak magnitude after the primary (deepest) minimum subtracted from the peak magnitude after the secondary minimum. From Figure 2 we derive that $\Delta B \sim \Delta V \sim \Delta R \sim + 0.05$. Furthermore, a closer inspection of the B curve reveals a small "shoulder" along the rise towards both the secondary maxima. This is possibly due to the ocurrence of starspots.

In fact, it is well-known that that EW variables are usually heavily spotted systems, as theoretically predicted by Binnendijk (1970). He was the first to propose that dark spots exist on the surfaces of the components to explain the asymmetry and variability of the light curves at different epochs. This hypothesis was later demonstrated by Doppler imaging (see for instance Hendry and Mochnacki 2000). One of the authors of the present paper already dealt with this issue and detected the presence of starspots in light curves taken at different epochs of one EW variable with an orbital period of ~0.355 day (Damasso *et al.* 2011).

Starspots are a possible explanation of the O'Connell Effect as well, but there is much uncertainty in this respect (Wilsey and Beaky 2009).

It would be interesting to collect new data of this system at different epochs to put in evidence possible evolutions that our data, taken during a single night, cannot reveal. In particular, short-period systems like ours can show variations in period or in the shape of the light curves, like an inversion of the primary and secondary maxima leading to an O'Connell Effect with opposite sign (see for example the case of V523 Cas treated in Zhang and Zhang 2004).

Let us now turn to the discussion of the spectroscopic data. The spectra in Figure 4 display the typical shape of K stars, without any evident superposition of different spectral types. This suggests that both components have similar spectra and surface temperatures. This is in accordance with the fact that the minima in the light curves are almost equal in deepness.

W UMa binaries are expected to be located within or in proximity of the main sequence stars (Bilir *et al.* 2005). This can be confirmed by our spectra: the prominence of the MgH band around 5200 Å and the tooth-shaped MgH feature around 4770 Å strongly suggest that the stars are dwarfs (Gray and Corbally 2009, p. 262).

To obtain a more precise classification, we resorted to the lines highlighted in Figure 4(c): the CaI line at 6162 Å, the BaII-FeI-CaI blend at 6497 Å, and the Hα line at 6563 Å. The latter directly correlates with temperature, while the first two inversely correlate with temperature, so that the CaI or BaII-FeI-CaI blend to Hα ratio is a useful temperature indicator.

Although in late-type stars it is often difficult to spot out an actual continuum to refer to, we calculated the equivalent widths of these three lines which are only indicative. They are:

$W\lambda$ (CaI) = 1.7 Å
$W\lambda$ (blend) = 0.8 Å
$W\lambda$ (Hα) = 0.4 Å

We decided to compare our spectra to the ones tabulated by Allen and Strom (1995) because they possess a spectral coverage and resolution quite similar to ours. The CaI to Hα ratio suggest a dK4 classification.

A further clue as to how to classify the two stars can be given by the slight difference in depth of the two minima. Such difference is nearly equal to 0.05 magnitude, that is, ~4.7% in flux. Calling $T_{1,2}$ the surface temperatures of the two components we can roughly infer that $(T_1 / T_2)^4 \sim 1.047 \rightarrow T_1 / T_2 \sim 1.012$, that is, the component 1 is hotter than the component 2 by 1.2 %. At temperatures between 4000 and 5000 K this means a difference of ~50 K. Unfortunately, the surface temperature of lower main sequence stars is not easy to calculate and within a same spectral type there can be a variance of more than 100 K (see for example Casagrande *et al.* 2006). Hence, the calculated temperature

difference cannot be safely assumed as to testify a difference of spectral type between the two components. In the end, we rest upon a dK4 classification for both components. In addition, this conclusion is consistent with a classification based on the color indices: according to Cox (2000) a dK4 star is expected to have $J–H = 0.58$ and $H–K = 0.11$, and our variable has $J–H = 0.583$ and $H–K = 0.125$.

Furthermore, we can try to deduce the masses of the two stars. If we call *a* the overall semi-major axis of the system (that is, the sum of the two semi-major axes with respect to the center of mass) expressed in AUs, T the period expressed in years, and $M_{1,2}$ the masses of the two components expressed in solar units, we have:

$$a^3 = T^2(M_1 + M_2) \quad (5)$$

From our photometric data we deduce $T = 0.238$ day $= 6.516 \times 10^{-4}$ yr. A mid-K dwarf typically has a mass $M \sim 0.7 – 0.75$; assuming $M_1 + M_2 = 1.45$, it results that $a \sim 1.27 \times 10^6$ km.

Assuming both components to have a radius R 0.75 – 0.8 with respect to the Sun, that is, about 5×10^5 km, we have a ~2.5R. This is fine because W UMa variables are supposed to be almost touching each other.

Moreover, one could ask how large a Doppler broadening such an orbital pattern would entail in spectra. Let us assume a circular orbit. At the time of maximum in the light curve we should have an overall Doppler broadening of the order of:

$$\Delta\lambda / \lambda = v / c = 2\pi a / (T_c) = 1.29 \times 10^{-3} \quad (6)$$

If we consider the Hα line at 6563Å we have that $\Delta\lambda \sim 8$ Å, that is, the width of the line should extend about from 6554.5 to 6571.5Å. If we consider the CaI line at 6162 we have $\Delta\lambda$ 8Å, that is, the width of the line should extend about from 6154 to 6170Å. These values are consistent with our spectra, but because of the low dispersion we can attain we believe we cannot draw any sure conclusion in this respect.

We finally looked for possible activity indicators in the spectra like emission lines, but we found none at the level of resolution accessible to us.

4. Acknowledgements

Authors Damasso, Cenadelli, and Calcidese are supported by grants provided by the European Union, the Autonomous Region of the Aosta Valley and the Italian Department for Work, Health and Pensions. The OAVdA is supported by the Regional Government of the Aosta Valley, the Town Municipality of Nus and the Mont Emilius Community. The telescope which led to the discovery of the variable star has been funded by the Fondazione Cassa di Risparmio di Torino (CRT). This

research has made use of the SIMBAD database, operated at CDS, Strasbourg, France, and of the NASA Astrophysics Data System Bibliographic Services.

References

AAVSO. 2012, APASS: The AAVSO Photometric All-Sky Survey (http://www.aavso.org/apass), AAVSO, Cambridge, MA.

Allen, L. E., and Strom, K. 1995, *Astron. J.*, **109**, 1379.

Bilir, S., Karataş, Y., Demircan, O., Eker, Z. 2005, *Mon. Not. Roy. Astron. Soc.*, **357**, 497.

Binnendijk, L. 1970, *Vistas Astron.*, **12**, 217.

Casagrande, L., Portinari, L., and Flynn, C. 2006, *Mon. Not. Roy. Astron. Soc.*, **373**, 13.

Cox, A. N. 2000, *Allen's Astrophysical Quantities*, 4th ed., Springer, New York.

Damasso, M., *et al.* 2010, *Publ. Astron. Soc. Pacific*, **122**, 1077.

Damasso, M., *et al.* 2011, *Open Eur. J. Var. Stars*, No. 138, 1.

Davidge, T. J., and Milone, E. F. 1984, *Astrophys. J., Suppl. Ser.*, **55**, 571.

Giacobbe, P., *et al.* 2012, *Mon. Not. Roy. Astron. Soc.*, **424**, 3101.

Gray, R. O., and Corbally, C. J. 2009, *Stellar Spectral Classification*, Princeton Univ. Press, Princeton, NJ.

Hendry, P. D., and Mochnacki, S. W. 2000, *Astrophys. J.*, **531**, 467.

Kidger, M. R. 2003, "The USNO A2.0 photometric scale compared to the standard Landolt BVR magnitudes" (http://quasars.org/docs/USNO_Landolt.htm, accessed April 2012).

Miller, V. R., Albrow, M. D., Afonso, C., and Henning, T. 2010, *Astron. Astrophys.*, **519A**, 12.

Monet, D. *et al.* 1998, *USNO-A V2.0 Catalog of Astrometric Standards,* U.S. Naval Observatory, Flagstaff, AZ.

Norton, A. J., *et al.* 2011, *Astron. Astrophys.*, **528A**, 90.

Palmer, D. M. 2009, *Astrophys. J.*, **695**, 496.

Pavlov, H. 2009, "Deriving a V magnitude From UCAC3" (http://www.hristopavlov.net/Articles/index.html).

Rucinski, S. M. 2006, *Mon. Not. Roy. Astron. Soc.*, **368**, 1319.

Skrutskie, M. F., *et al.* 2006, *The Two Micron All Sky Survey, Astron. J.,* **131**, 1163.

U.S. Naval Observatory. 2012, *UCAC-3* (http://www.usno.navy.mil/USNO/astrometry/optical-IR-prod/ucac).

Weldrake, D. T. F., Sackett, P. D., and Bridges, T. J. 2007, *Astron. J.*, **133**, 1447.

Wilsey, N. J., and Beaky, M. M. 2009, in *The Society for Astronomical Sciences 28th Annual Symposium on Telescope Science* (May 19–21, 2009), Soc. Astron. Sci., Rancho Cucamonga, CA, 107.

Zhang, X.B., and Zhang, R.X. 2004, *Mon. Not. Roy. Astron. Soc.*, **347**, 307.

Table 1. Optical configurations used to acquire the spectra of the variable.

Configuration	*Spectral coverage*	*Mean dispersion*	*Resolution*
grism3	~3700 – ~5850Å	~2.1Å/px	~650
grism8	~5950 – ~8000Å	~2.0Å/px	~1900

Table 2. Comparison stars used for differential photometry in B, V, and R bands.

Star	*R.A.* *h m s*	*Dec.* ° ′ ″	*Band*
UCAC-3 320-037770	07 09 19.041	+69 55 06.66	B V
UCAC-3 320-037772	07 09 21.093	+69 56 00.27	B
UCAC-3 320-037776	07 09 24.095	+69 56 59.02	B V R
UCAC-3 320-037779	07 09 28.970	+69 51 43.34	B R
UCAC-3 320-037783	07 09 32.398	+69 50 57.44	B
UCAC-3 320-037784	07 09 32.649	+69 58 42.06	B
UCAC-3 320-037787	07 09 34.315	+69 49 49.11	B V R
UCAC-3 320-037794	07 09 42.534	+69 50 59.13	B
UCAC-3 320-037795	07 09 43.173	+69 54 42.21	B
UCAC-3 320-037798	07 09 45.939	+69 55 15.41	B
UCAC-3 320-037799	07 09 47.551	+69 52 26.48	B
UCAC-3 320-037820	07 10 09.948	+69 55 17.80	B
UCAC-3 320-037821	07 10 11.189	+69 50 45.90	B
UCAC-3 320-037823	07 10 14.455	+69 50 34.28	R
UCAC-3 320-037827	07 10 20.912	+69 49 40.04	B V R
UCAC-3 320-037828	07 10 21.806	+69 52 30.72	B
UCAC-3 320-037831	07 10 23.959	+69 51 24.78	B R
UCAC-3 320-037835	07 10 31.401	+69 53 52.17	B
UCAC-3 320-037849	07 10 38.339	+69 57 18.61	B
UCAC-3 320-037857	07 10 42.666	+69 49 14.61	B
UCAC-3 320-037860	07 10 44.576	+69 51 52.55	B
UCAC-3 320-037862	07 10 47.011	+69 51 35.23	B
UCAC-3 320-037867	07 10 54.909	+69 52 17.17	B V R
UCAC-3 320-037871	07 11 03.636	+69 52 31.88	B
UCAC-3 320-037876	07 11 07.800	+69 51 27.49	B V
UCAC-3 320-037881	07 11 10.879	+69 51 29.52	B V
UCAC-3 320-037885	07 11 14.572	+69 56 07.65	B V R
UCAC-3 320-037896	07 11 27.544	+69 48 08.74	B
UCAC-3 320-037901	07 11 32.558	+69 52 03.82	B V R
2MASS 07110649+6947296	07 11 06.492	+69 47 29.61	B
2MASS 07094405+6952413	07 09 44.051	+69 52 41.40	B

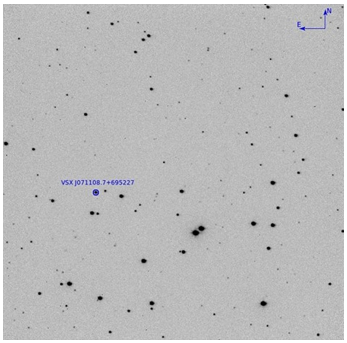

Figure 1. The star field of VSX J071108.7+695227, with the variable star target highlighted. The scale of the image is 16.5 × 16.5 arcmin^2. North is up and east is to the left.

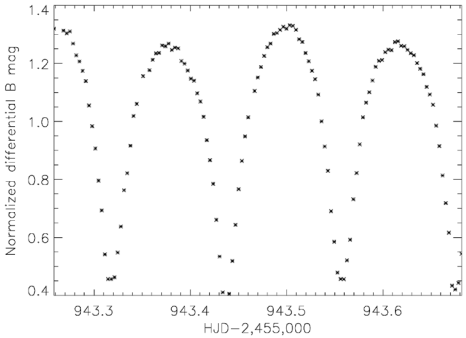

Figure 2a. Differential light curve of the variable star VSX J071108.7+695227 in B filter. The data were collected on January 16, 2012.

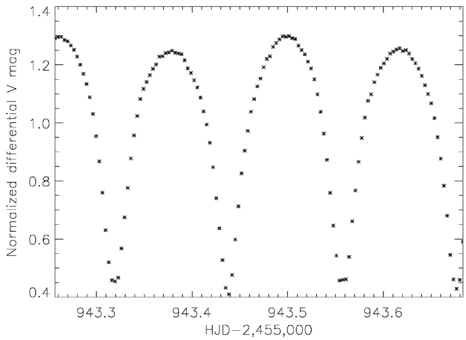

Figure 2b. Differential light curve of the variable star VSX J071108.7+695227 in V filter. The data were collected on January 16, 2012.

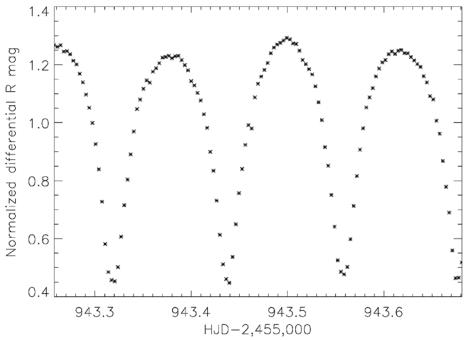

Figure 2c. Differential light curve of the variable star VSX J071108.7+695227 in R filter. The data were collected on January 16, 2012.

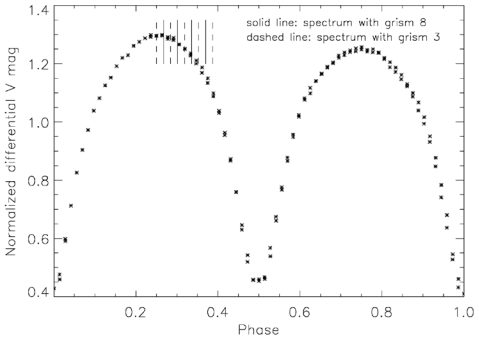

Figure 3. Differential light curve of VSX J071108.7+695227 in V band folded according to the orbital period ~0.238 days.

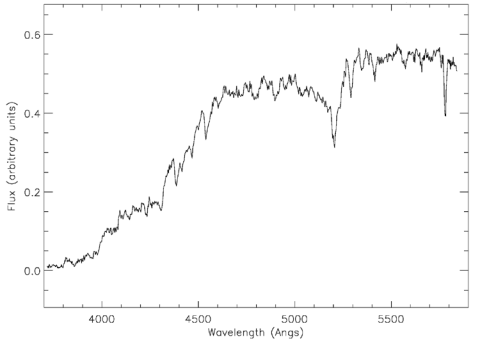

Figure 4a. Spectra of the variable star VSX J071108.7+695227 at maximum brightness, taken with grism3. The mid epoch of the exposure is HJD 2455953.493615.

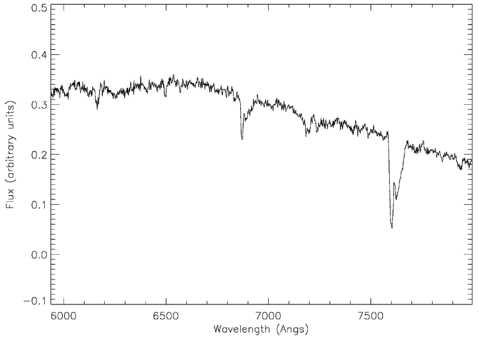

Figure 4b. Spectra of the variable star VSX J071108.7+695227 at maximum brightness, taken with grism8. A magnified region is displayed in Figure 4c. The mid epoch of the exposure is HJD 2455953.497677.

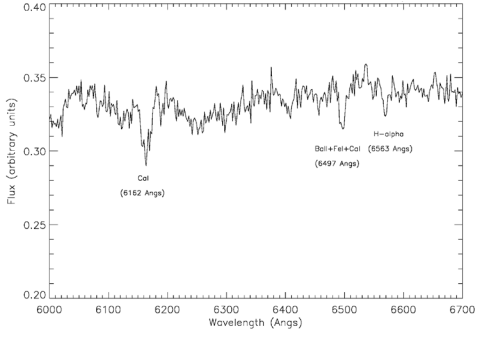

Figure 4c. A magnified region of the spectra of the variable star VSX J071108.7+695227 at maximum brightness, taken with grism8. The mid epoch of the exposure is HJD 2455953.497677.